

PAPER • OPEN ACCESS

Iron self diffusion in liquid pure iron and iron-carbon alloys

To cite this article: A Meyer *et al* 2019 *J. Phys.: Condens. Matter* **31** 395401

View the [article online](#) for updates and enhancements.




IOP | ebooks™

Bringing you innovative digital publishing with leading voices to create your essential collection of books in STEM research.

Start exploring the collection - download the first chapter of every title for free.

Iron self diffusion in liquid pure iron and iron-carbon alloys

A Meyer¹, L Hennig¹, F Kargl¹ and T Unruh^{2,3}

¹ Institut für Materialphysik im Weltraum, Deutsches Zentrum für Luft- und Raumfahrt (DLR), 51170 Köln, Germany

² Forschungsneutronenquelle Heinz Maier-Leibnitz (FRM II), Technische Universität München, 85747 Garching, Germany

E-mail: andreas.meyer@dlr.de

Received 23 April 2019, revised 28 May 2019

Accepted for publication 10 June 2019

Published 9 July 2019



Abstract

With incoherent quasielastic neutron scattering self-diffusion coefficients D_s in pure iron, and iron-carbon alloys containing 8.7 at% and 16.9 at% carbon have been measured. At the melting point D_s in liquid iron is $2.8(1) \times 10^{-9} \text{ m}^2 \text{ s}^{-1}$. For the close-to-eutectic $\text{Fe}_{83.1}\text{C}_{16.9}$ composition $D_s = 1.33(12) \times 10^{-9} \text{ m}^2 \text{ s}^{-1}$ at $T_{\text{liq}} = 1432 \text{ K}$. Contradicting conclusions drawn from literature values of tracer diffusion experiments the addition of carbon has only a minor effect on the iron mobility: at a given temperature the self-diffusion coefficient in $\text{Fe}_{83.1}\text{C}_{16.9}$ is only 10% larger than in liquid iron, although mixing has a drastic effect on liquidus temperature and phase behavior.


Keywords: self diffusion, liquid metal, liquid iron carbon, quasielastic neutron scattering

1. Introduction

The knowledge of mass transport properties in the liquid state plays a relevant role in the understanding and modeling of technological and geoscientific processes. In this context in recent years quasielastic neutron scattering has proven to be a versatile tool for the study of self diffusion in liquid metals and alloys at high temperatures. With incoherent quasielastic neutron scattering diffusive dynamics is probed on microscopic time and length scales that are unaffected by fluid flow in the liquid sample and thus, accurate self-diffusion coefficients can be measured on an absolute scale [1]. With these data some long standing issues could be addressed, e.g. the temperature dependence of self diffusion around the melting point [2, 3], the relation of viscous flow and atomic diffusion [4, 5], the relation of self- and interdiffusion [6–8], and the onset of glassy dynamics in viscous metallic melts [9–11].

Another important aspect of self diffusion in metallic liquids is to what extent the addition of a further alloying component is impacting the overall atomic mobility, which in turn poses a prerequisite for modeling of microstructure formation from the liquid or an understanding of vitrification, in general. In iron based systems applications are ranging from the description of solidification processes in cast iron and steels, where in most cases the liquid composition is changing during microstructure formation [12], to the prediction of transport properties of the Earth outer-core, that are fundamental for understanding its origin, evolution, and current dynamics and where experimental data are challenging to measure due to the high temperatures and pressures involved [13].

In metallic melts mixing often has a drastic effect on the thermodynamics, i.e. on the phase behavior and the liquidus temperature. However, in dense metallic liquids only a minor effect on the transport coefficient is found: for example in Ni-rich binary alloys the addition of 20 at% phosphorous [14] or of 25% aluminum [15] only has some 10% effect on the Ni self-diffusion coefficient at constant temperature. Reported data indicate a counter example: iron-carbon, where mixing would have a drastic effect on the iron self diffusion—if the values from tracer experiments in Fe–C alloys [16] and liquid iron [19] are accurate. Although liquid Fe–C exhibits a deep eutectic at 17.1 at% carbon [17], the self-diffusion coefficients

 Original content from this work may be used under the terms of the [Creative Commons Attribution 3.0 licence](https://creativecommons.org/licenses/by/3.0/). Any further distribution of this work must maintain attribution to the author(s) and the title of the work, journal citation and DOI.

³ Present address: Lehrstuhl für Kristallographie und Strukturphysik, Friedrich-Alexander-Universität Erlangen-Nürnberg, 91058 Erlangen, Germany

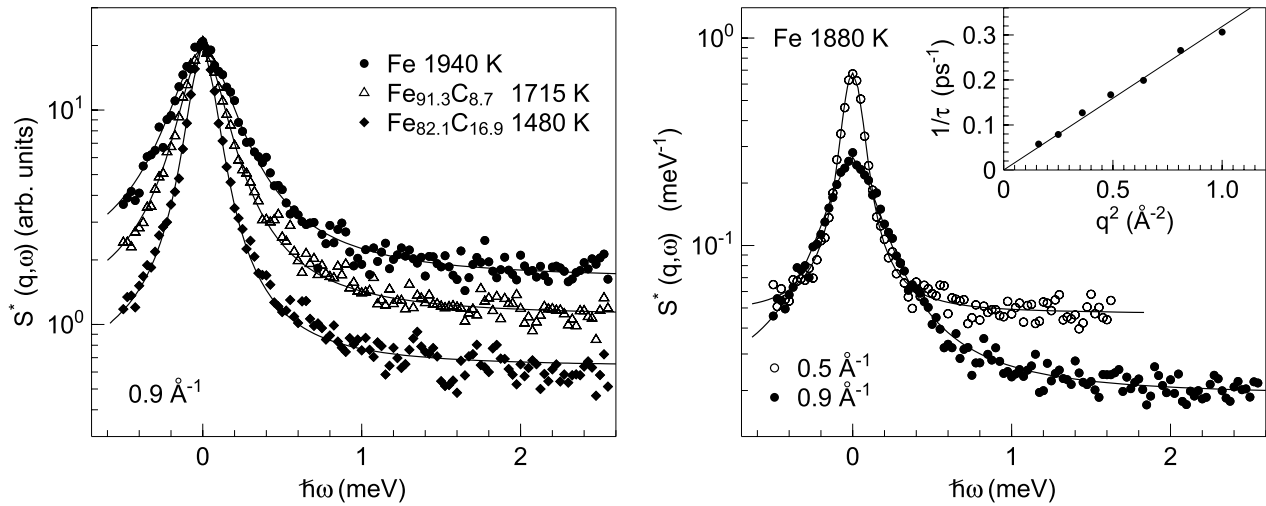


Figure 1. Left panel: quasielastic spectra of liquid Fe and Fe–C alloys at different temperatures—for a better representation normalized to the value of the iron spectrum at $S(q, \omega = 0)$. Spectra are dominated by incoherent scattering of the iron atoms. Solid lines are fits with equation (1). Right panel: quasielastic signal in liquid Fe at 1880 K. Toward small q an increasing contribution from magnetic scattering results in an increasing but flat contribution to the spectra. Solid lines are fits with equation (1). Inset: resulting relaxation times τ_q are rescaled according to $1/\tau = D_s q^2$.

of Fe in $\text{Fe}_{84}\text{C}_{16}$ and Fe_{94}C_6 are about $7\text{--}9 \times 10^{-9} \text{ m}^2 \text{ s}^{-1}$ at 1600 K [16], significantly above the values of pure iron from molecular dynamics computer simulations with various interaction potentials [18] that are in the range of $2.7\text{--}3.6 \times 10^{-9} \text{ m}^2 \text{ s}^{-1}$ at 1833 K. Experimental self-diffusion coefficients for pure liquid iron have been reported at somewhat elevated pressure: at 2 GPa and at 1883 K the value reads as low as $0.8 \times 10^{-9} \text{ m}^2 \text{ s}^{-1}$ [19].

As has been shown recently by *in situ* monitoring of liquid interdiffusion processes with x-ray radiography on binary alloys, data from classical long-capillary diffusion experiments are severely hampered by melting and solidification of the samples, as well as by convective flow during annealing. This leads to systematic errors that can be as large as several 100% [20]. Beside a time-resolved measurement of the diffusion process, a sufficiently large difference in density of the diffusion couple can suppress convective flow and, hence, is a prerequisite for accurate measurements [6–8]. However, this can not be realized for tracer diffusion into an homogenous liquid, as has been done in [16, 19] and it does not apply to one-component liquids: in liquid Cu, self-diffusion coefficients measured with quasielastic neutron scattering [21] are significantly smaller than those from previous long-capillary tracer experiments [22].

2. Experimental

In order to study the impact of carbon addition on the atomic mobility of the iron atoms, we measured iron self-diffusion coefficients in pure liquid iron and liquid $\text{Fe}_{91.3}\text{C}_{8.7}$ and $\text{Fe}_{83.1}\text{C}_{16.9}$ alloys that contain 2.0 wt% and 4.2 wt% carbon respectively. The samples were made from an ARMCO iron ingot (HKM-Stahl GmbH) of 99.9 wt% metallic purity and Graphite KS 75 (LONZA) powder of 99.9 wt% purity. The Fe–C alloys were prepared with induction melting of pure

iron with the graphite powder under Argon atmosphere. The liquidus temperature of the $\text{Fe}_{83.1}\text{C}_{16.9}$ alloy was measured with differential scanning calorimetry applying several runs with different heating rates. The resulting liquidus is $1432 \pm 3 \text{ K}$ in excellent agreement with the liquidus temperature of the eutectic composition at 17.1 at% carbon content at 1426 K [17].

The liquid samples were measured at the neutron time-of-flight spectrometer ToFToF [23, 24] at the Heinz Maier-Leibnitz neutron source (FRM II). The setup with a wavelength of the incident neutrons of $\lambda = 7 \text{ \AA}$ gives an accessible wave-number range q of about $0.4\text{--}1.6 \text{ \AA}^{-1}$ at zero energy transfer at an instrumental energy resolution of about 70 \mu eV at full width half maximum. For the neutron time-of-flight experiment a Al_2O_3 container with 0.5 mm wall thickness was used giving a cylindrical sample geometry of the liquid samples of 9 mm in diameter and of 40 mm in height. The samples were annealed in a Nb electrical resistance furnace that provides a temperature stability of better than 0.5 K along the sample. Spectra of pure iron were taken at temperatures ranging from 1820 K to 1940 K in steps of 30 K and for 20 min at each temperature. For the Fe–C alloys measurement times were 30 min at each temperature. Mass loss for all samples was well below 0.1%.

A measurement of a sample with pure Vanadium foils rolled into an empty Al_2O_3 container at a temperature of 295 K served as the instrumental energy resolution function of the spectrometer. Data were analyzed using the Frida software [25]. Measured time-of-flight spectra were normalized to the Vanadium standard, corrected for self absorption and empty container scattering, and interpolated to constant wave numbers q . Spectra are shown in figure 1.

The spectra are fitted in the quasielastic regime with the Fourier transform of the Kohlrausch stretched exponential function convoluted with the instrumental resolution function:

$$S^*(q, \omega) = b_q + R(q, \omega) \otimes S(q, \omega), \quad (1)$$

where $R(q, \omega)$ denotes the instrumental energy resolution function, b_q a q dependent constant contribution to the quasi-elastic signal, and $S(q, \omega)$ the scattering law:

$$S(q, \omega) = A_q \int dt e^{-i\omega t} \exp[-(t/\tau_q)^{\beta_q}]. \quad (2)$$

A_q is an amplitude of the structural relaxation, τ_q its relaxation time, and β_q a stretching exponent. The data for all three samples and at all temperatures are best described with a stretching exponent of $\beta_q = 1.0$, which corresponds to a single Lorentz function for the scattering law $S(q, \omega)$. This is in line with theoretical predictions in the hydrodynamic limit at small q [26], and is equally found in other pure metallic liquids [1, 2, 21, 27] and binary liquid alloys in the investigated dynamic regime of relaxation time and momentum transfer [15, 28, 29]. Only for glass-forming metallic alloys and in a dynamic range that corresponds to self-diffusion coefficients well below $10^{-9} \text{ m}^2 \text{ s}^{-1}$, the onset of glassy dynamics results in a deviation from an exponential decay, $\beta_q < 1.0$ [5, 9].

Iron has an incoherent scattering cross section of 0.4 barn and a coherent scattering cross section of 11.6 barn—carbon of 0.0001 and 5.56 respectively [30]. It has been shown in general for liquid metals, that in the intermediate q range investigated here, coherent scattering contributions to the quasielastic signal are well accounted for by the energy independent contribution b_q [1]. In addition to the aforementioned coherent contributions to $S(q, \omega)$ from density fluctuations, neutron scattering on liquid iron and iron-carbon alloys exhibits a magnetic scattering contribution from spin dynamics of the iron atoms. This dynamics is fast compared with the diffusive motion of the atoms and shows itself merely in an increasing b_q towards small q values (figure 1).

Therefore, the structural relaxation dynamics in $S(q, \omega)$ is dominated by incoherent scattering contributions of iron. The inset in the right panel of figure 1 displays resulting relaxation times τ_q from fits with equation (1). The data are rescaled according to $1/\tau_q = D_s q^2$, where D_s denotes the self-diffusion coefficient [26]. The $1/q^2$ scaling again confirms that the relaxation is dominated by incoherent scattering. Hence, following the arguments above, D_s represents the iron self-diffusion coefficient.

3. Results and discussion

The resulting iron self-diffusion coefficients are shown in figure 2 as a function of temperature. Values range from $(3.56 \pm 0.12) \times 10^{-9} \text{ m}^2 \text{ s}^{-1}$ at 1940 K in liquid iron to $(1.53 \pm 0.13) \times 10^{-9} \text{ m}^2 \text{ s}^{-1}$ at 1480 K in liquid $\text{Fe}_{83.1}\text{C}_{16.9}$ (table A1). The temperature dependence of D_s is best described with an Arrhenius behavior:

$$D = D_0 \exp(-E_A/k_B T), \quad (3)$$

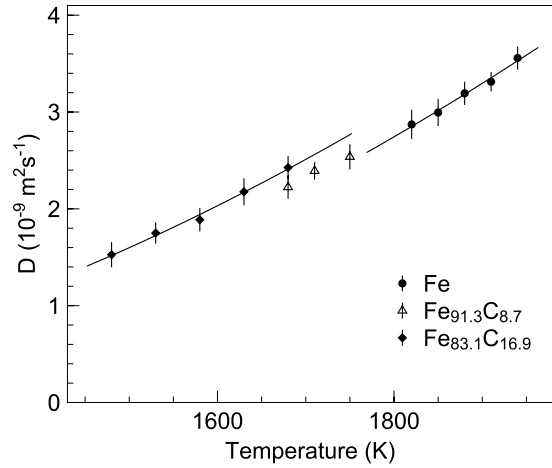


Figure 2. Iron self-diffusion coefficients in liquid Fe and Fe–C alloys as measured with quasielastic neutron scattering. The addition of carbon only has a minor effect on the iron mobility in the liquid. Lines are Arrhenius-fits with equation (3).

with a pre-factor D_0 and an activation energy E_A . $k_B = 8.617 \times 10^{-2} \text{ meV K}^{-1}$ is the Boltzmann constant. A best fit to the diffusion coefficients of pure iron gives $E_A = (540 \pm 34) \text{ meV}$ per atom and a $D_0 = (89 \pm 9) \times 10^{-9} \text{ m}^2 \text{ s}^{-1}$. For liquid $\text{Fe}_{83.1}\text{C}_{16.9}$ data are $E_A = (496 \pm 26) \text{ meV}$ per atom and a $D_0 = (74 \pm 7) \times 10^{-9} \text{ m}^2 \text{ s}^{-1}$. Diffusion coefficients for the $\text{Fe}_{91.3}\text{C}_{8.7}$ alloy are in between the values for liquid iron and $\text{Fe}_{83.1}\text{C}_{16.9}$. As compared to liquid iron, in liquid nickel the activation energy with a value of $E_A = (470 \pm 30) \text{ meV}$ and the pre-factor with a value of $D_0 = (77 \pm 8) \times 10^{-9} \text{ m}^2 \text{ s}^{-1}$ are similar [2], whereas values in liquid copper [21] are slightly smaller: $E_A = (337 \pm 5) \text{ meV}$ per atom and a $D_0 = (58.7 \pm 3) \times 10^{-9} \text{ m}^2 \text{ s}^{-1}$.

Figure 3 displays the data from quasielastic neutron scattering as compared to tracer data in Fe–C [16] and pure iron [19], as well as a prediction for iron self diffusivity from theory [31]. Dobson [19] reported a value from a tracer experiment in liquid iron at 2 GPa pressure that is well below $10^{-9} \text{ m}^2 \text{ s}^{-1}$ at 1883 K. As compared to the iron self-diffusion coefficients presented here, and taking into account the small compressibility in liquid iron [32], the impact of pressure on the atomic mobility would be unexpectedly large, and hence the reported value appears to be at least a factor of 3 too small. Tracer data from Yang *et al* in liquid Fe–C are a factor of about 4 larger than the data from quasielastic neutron scattering.

At the respective melting temperature the self-diffusion coefficient in liquid Fe ($2.8(1) \times 10^{-9} \text{ m}^2 \text{ s}^{-1}$) is slightly smaller than that in liquid Ni ($3.28(7) \times 10^{-9} \text{ m}^2 \text{ s}^{-1}$). Protopapas *et al* presented a theory of transport in liquid metals based upon the assumptions that liquid metals can be treated as a hard-sphere fluid and mass transport is accurately described by the Enskog theory plus corrections obtained from molecular dynamics simulations [31]. In their seminal paper, predictions for self-diffusion coefficients of some liquid metals were listed including Ni and Fe. In liquid Ni values are

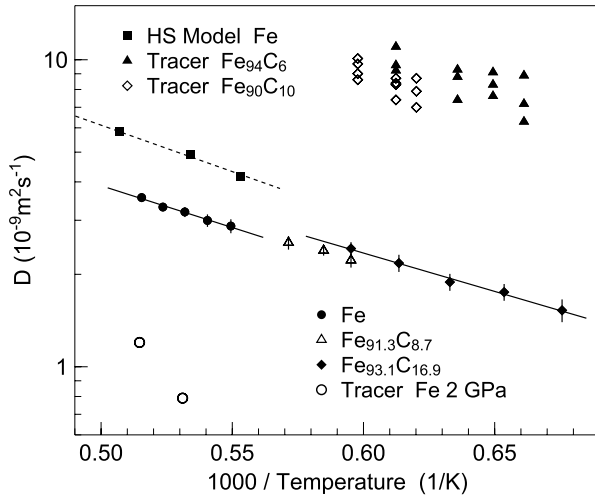


Figure 3. Arrhenius plot of iron self-diffusion coefficients in liquid Fe and Fe–C. Tracer data in Fe–C from [16], tracer data in Fe from [19], and theoretical prediction from [31]. Lines are fits with equation (3).

overestimated in their theory by about 20%. In liquid iron the deviation from prediction is already about 50% and also the activation energy $E_A = 600$ meV is larger than that from the quasielastic neutron scattering data. Figure 3 emphasizes the necessity for measurements of accurate transport coefficients for the further development of theoretical models.

As has been demonstrated on Ti [27] and Ni–Zr [33] experimental self-diffusion coefficients in the liquid state are a vital input for the improvement of interatomic potentials used in molecular dynamics (MD) simulations in the liquid: a calibration of interaction potentials with accurate self-diffusion coefficients resulted in a realistic modeling of various melt properties, including the location of the melting transition and the liquid density. In this context, accurate self-diffusion coefficients in liquid iron and iron-carbon can aid the development of interatomic potentials [18] to explore a range of temperature and pressure, that is otherwise challenging to obtain experimentally: e.g. the study of mass transport coefficients in liquid iron up to Earth-core pressures and temperatures with computer simulation [34, 35].

For the close-to-eutectic $\text{Fe}_{83.1}\text{C}_{16.9}$ composition $D_s \simeq 1.3 \times 10^{-9} \text{ m}^2 \text{ s}^{-1}$ at $T_{\text{liq}} = 1432$ K. The addition of carbon has only a minor effect on the iron mobility in the liquid: at a given temperature the iron self-diffusion coefficient in $\text{Fe}_{83.1}\text{C}_{16.9}$ is only about 10% larger than that in liquid iron. Values around and below $10^{-9} \text{ m}^2 \text{ s}^{-1}$ at the liquidus temperature are typically found in glass-forming multi-component metallic melts [9, 11] or in binary liquid alloys at compositions around deep eutectics [3]. A similar behaviour is found

in liquid Ni and $\text{Ni}_{80}\text{P}_{20}$: the addition of phosphorous causes a decrease in the liquidus temperature of 556 K (1727 K in pure Ni, 1171 K in $\text{Ni}_{80}\text{P}_{20}$), whereas the Ni self-diffusion coefficient at a given temperature is only increasing by about 10% [2, 14]. This comes along with a similar dense packing of the atoms in both Ni and $\text{Ni}_{80}\text{P}_{20}$.

In Ni and $\text{Ni}_{80}\text{P}_{20}$ the packing fraction, that is some 0.51 at the melting point of Ni (1727 K) for both systems [14]. The density of liquid iron at the melting temperature is 7.035 g cm^{-3} [36] and that of $\text{Fe}_{83.1}\text{C}_{16.9}$ at 1811 K is 6.79 g cm^{-3} [37]. Using the same procedure as in [14] to estimate the packing fraction in liquid Fe and $\text{Fe}_{83.1}\text{C}_{16.9}$ with a covalent radius of $1.17 \times 10^{-8} \text{ cm}$ of Fe and a covalent radius of $0.77 \times 10^{-8} \text{ cm}$ of C, results in a packing fraction of 0.509 for liquid iron and a value of 0.50 for liquid $\text{Fe}_{83.1}\text{C}_{16.9}$ that are equal within error bars. It appears that mixing at constant packing fraction leads to similar diffusive dynamics also in densely-packed liquid iron and iron-carbon alloys.

4. Conclusion

In conclusion, we provide iron self-diffusion data for liquid iron, $\text{Fe}_{91.3}\text{C}_{8.7}$, and $\text{Fe}_{83.1}\text{C}_{16.9}$. With these, we show that previous literature values from tracer experiments using a long-capillary set-up in Fe–C [16] are off by a factor of 4 and using a pressure cell in liquid iron [19] are smaller than factor of about 4 (figure 3). In contrast, the conclusions drawn from the previous data sets, that the addition of carbon causes a strong mixing effect on the dynamics in the melt, is not supported: the addition of carbon to iron has only a 10% effect on the iron mobility in the liquid. Furthermore, there is no correlation between the value of the self-diffusion coefficient at the liquidus temperature and the onset of glassy dynamics: although the diffusion coefficients in the close-to-eutectic $\text{Fe}_{83.1}\text{C}_{16.9}$ approach a value of $10^{-9} \text{ m}^2 \text{ s}^{-1}$, no onset of glassy dynamics, i.e. a deviation from an Arrhenius-type temperature dependence of the self-diffusion coefficient or a deviation from a Lorentz-type quasielastic signal could be observed. Quasielastic neutron scattering measurements upon mixing other light elements (e.g. sulfur, boron, and silicon) to liquid iron and nickel are in preparation in order to clarify how generic these findings are.

Acknowledgment

We thank Thomas Voigtmann for a critical reading of the manuscript.

Appendix. Iron self-diffusion coefficients

Table A1. Iron self diffusion coefficients in liquid Fe and Fe–C alloys as measured by quasielastic neutron scattering.

	T (K)	D ($10^{-9} \text{ m}^2\text{s}^{-1}$)
Pure Fe	1820 ± 2	2.93 ± 0.15
	1850 ± 2	2.99 ± 0.14
	1880 ± 2	3.19 ± 0.12
	1910 ± 2	3.31 ± 0.10
	1940 ± 2	3.56 ± 0.12
Fe _{91.3} C _{8.7}	1680 ± 2	2.22 ± 0.12
	1715 ± 2	2.39 ± 0.09
	1750 ± 2	2.54 ± 0.13
Fe _{83.1} C _{16.9}	1480 ± 2	1.53 ± 0.13
	1530 ± 2	1.75 ± 0.11
	1580 ± 2	1.89 ± 0.12
	1630 ± 2	2.18 ± 0.14
	1680 ± 2	2.43 ± 0.12

ORCID iDs

A Meyer  <https://orcid.org/0000-0002-0604-5467>

References

- [1] Meyer A 2015 *EPJ Web Conf.* **83** 1002
- [2] Meyer A, Holland-Moritz D, Heinen O and Unruh T 2008 *Phys. Rev. B* **77** 092201
- [3] Kordel T, Holland-Moritz D, Yang F, Peters J, Unruh T, Hansen T and Meyer A 2011 *Phys. Rev. B* **83** 104205
- [4] Brillo J, Pommrich A I and Meyer A 2011 *Phys. Rev. Lett.* **107** 165902
- [5] Yang F, Unruh T and Meyer A 2014 *Europhys. Lett.* **107** 26001
- [6] Sondermann E, Kargl F and Meyer A 2016 *Phys. Rev. B* **93** 184201
- [7] Yang F, Heintzmann P, Kargl F, Binder K, Nowak B, Schillinger B, Voigtmann T and Meyer A 2018 *Phys. Rev. B* **98** 064202
- [8] Sondermann E, Jakse N, Binder K, Mielke A, Heuskin D, Kargl F and Meyer A 2019 *Phys. Rev. B* **99** 024204
- [9] Meyer A 2002 *Phys. Rev. B* **66** 134205
- [10] Basuki S W, Yang F, Gill E, Rätzke K, Meyer A and Faupel F 2017 *Phys. Rev. B* **95** 024301
- [11] Jonas I, Yang F and Meyer A *Phys. Rev. Lett.* in preparation
- [12] Stefanescu D M 2006 *ISIJ Int.* **46** 786
- [13] Dobson D P and Wiedenbeck M 2002 *Geophys. Res. Lett.* **29** 015536
- [14] Mavila Chathoth S, Meyer A, Schober H and Juranyi F 2004 *Appl. Phys. Lett.* **85** 4881
- [15] Stüber S, Holland-Moritz D, Unruh T and Meyer A 2010 *Phys. Rev. B* **81** 024204
- [16] Yang L, Simnad M T and Derge G 1956 *JOM* **8** 1577
- [17] Massalski T B and Okamoto H 1990 *Binary Alloy Phase Diagrams* (Materials Park, OH: ASM International)
- [18] Sobolev A, Starukhin V, Buldashev I and Mirzoev A 2017 *EPJ Web Conf.* 151 05004
- [19] Dobson D P 2002 *Phys. Earth Planet. Inter.* **130** 271
- [20] Kargl F, Sondermann E, Weis H and Meyer A 2013 *High Temp. High Press.* **42** 3
- [21] Meyer A 2010 *Phys. Rev. B* **81** 012102
- [22] Henderson J and Yang L 1961 *Trans. Met. Soc. AIME* **221** 72
- [23] Unruh T, Meyer A, Neuhaus J and Petry W 2007 *Neutron News* **18** 22
- [24] Unruh T, Neuhaus J and Petry W 2007 *Nucl. Instrum. Methods A* **580** 1414
- [25] FRIDA-1: (<http://sourceforge.net/projects/frida>)
- [26] Boon J P and Yip S 1980 *Molecular Hydrodynamics* (New York: McGraw-Hill)
- [27] Horbach J, Rozas R E, Unruh T and Meyer A 2009 *Phys. Rev. B* **80** 212203
- [28] Brillo J, Mavila Chathoth S, Koza M M and Meyer A 2008 *Appl. Phys. Lett.* **93** 121905
- [29] Pommrich A I, Meyer A, Holland-Moritz D and Unruh T 2008 *Appl. Phys. Lett.* **92** 241922
- [30] Koester L, Rauch H and Seymann E 1991 *At. Data Nucl. Data Tables* **49** 65
- [31] Protopapas P, Andersen H C and Parlee N A D 1973 *J. Chem. Phys.* **59** 15
- [32] Sanloup C, Guyot F, Gillet P, Fiquet G, Hemley R J, Mezoua M and Martinez I 2000 *Europhys. Lett.* **52** 151
- [33] Kuhn P, Horbach J, Kargl F, Meyer A and Voigtmann T 2014 *Phys. Rev. B* **90** 024309
- [34] Cao Q-L, Wang P-P, Huang D-H, Yang J-S, Wan M-J and Wang F-H 2014 *J. Chem. Phys.* **140** 114505
- [35] Wagle F and Steinle-Neumann G 2019 *J. Geophys. Res.: Solid Earth* **124** 1
- [36] Assael M J et al 2006 *J. Phys. Chem. Ref. Data* **35** 285
- [37] Jimbo I and Cramb A W 1993 *Metall. Trans. B* **24** 5